THE JOURNAL OF BIOLOGICAL CHEMISTRY VOL. 289, NO. 30, pp. 20858–20870, July 25, 2014

Mammalian COPII Coat Component SEC24C Is Required for Embryonic Development in Mice*

Received for publication, April 15, 2014, and in revised form, May 28, 2014 Published, JBC Papers in Press, May 29, 2014, DOI 10.1074/jbc.M114.566687

Elizabeth J. Adams[‡§1], **Xiao-Wei Chen**[‡], **K. Sue O'Shea**[¶], **and David Ginsburg**[‡§‖**2]

From the [‡]*Life Sciences Institute,* [§]*Program in Cellular and Molecular Biology, Departments of* [¶]*Cell and Developmental Biology and* [‖]*Internal Medicine, Human Genetics, and Pediatrics,* [**]*Howard Hughes Medical Institute, University of Michigan, Ann Arbor, Michigan 48109*

Background: SEC24 is responsible for selectively recruiting cargo proteins into COPII vesicles.
Results: Mice completely lacking one of the four SEC24 paralogs (SEC24C) die early in post-implantation embryonic development.
Conclusion: SEC24C is essential for embryonic development but is dispensable in a number of cell types.
Significance: These findings provide new insight into the function of SEC24C *in vivo*.

COPII-coated vesicles mediate the transport of newly synthesized proteins from the endoplasmic reticulum to the Golgi. SEC24 is the COPII component primarily responsible for recruitment of protein cargoes into nascent vesicles. There are four *Sec24* paralogs in mammals, with mice deficient in SEC24A, -B, and -D exhibiting a wide range of phenotypes. We now report the characterization of mice with deficiency in the fourth *Sec24* paralog, SEC24C. Although mice haploinsufficient for *Sec24c* exhibit no apparent abnormalities, homozygous deficiency results in embryonic lethality at approximately embryonic day 7. Tissue-specific deletion of *Sec24c* in hepatocytes, pancreatic cells, smooth muscle cells, and intestinal epithelial cells results in phenotypically normal mice. Thus, SEC24C is required in early mammalian development but is dispensable in a number of tissues, likely as a result of compensation by other *Sec24* paralogs. The embryonic lethality resulting from loss of SEC24C occurs considerably later than the lethality previously observed in SEC24D deficiency; it is clearly distinct from the restricted neural tube phenotype of *Sec24b* null embryos and the mild hypocholesterolemic phenotype of adult *Sec24a* null mice. Taken together, these results demonstrate that the four *Sec24* paralogs have developed unique functions over the course of vertebrate evolution.

Approximately one-third of all mammalian proteins traverse the secretory pathway en route to their final destinations, including cell surface membranes and intracellular compartments, as well as the extracellular space (1, 2). These proteins begin their journey in the endoplasmic reticulum (ER),[3] where they are recruited into newly forming COPII vesicles located at ribosome-free ER exit sites (3, 4). The COPII vesicles containing these cargoes are then trafficked from the ER to the ER-Golgi intermediate compartment.

The mechanism of COPII coat assembly has been elegantly dissected in *Saccharomyces cerevisiae,* and the fundamental mechanisms appear to be conserved from yeast to humans (5). Vesicle formation is initiated with the activation of the small GTPase Sar1p by the GEF Sec12p, which is localized on the ER membrane. GTP binding to Sar1p induces a conformational change and insertion of a small amphipathic helix of Sar1p into the ER membrane and begins the process of vesicle formation (6, 7). Activated Sar1p recruits the Sec23p-Sec24p heterodimer to the ER, forming the inner layer of the COPII coat (8, 9). Polymerization of Sec13p and Sec31p heterotetramers to form the outer layer promotes further curvature and budding of the nascent COPII vesicle from the ER (10).

SEC24 is the COPII component thought to be primarily responsible for cargo recruitment, with ER exit motifs on protein cargoes interacting with specific binding sites on SEC24 (11, 12). SEC24-cargo interactions are either direct, in the case of transmembrane proteins, or require a transmembrane adaptor to mediate the interaction of ER luminal cargo with the COPII coat located on the cytoplasmic face of the ER membrane. Examples include the well characterized interaction between the adaptor component LMAN1/MCFD2 and its ER luminal cargoes Factor V and Factor VIII (13, 14).

In *S. cerevisiae*, loss of Sec24p is lethal, although deficiency of either of two nonessential Sec24p paralogs, Iss1p or Lst1p, results in specific cargo-transport defects (15). The mammalian genome encodes four paralogs of *Sec24* (*Sec24a–d*), which can be classified into two subgroups, SEC24A/B and SEC24C/D, based on protein sequence identity, with the A/B subgroup more closely related to the ancestral yeast paralog Sec24p (16, 17). All four paralogs contain a highly conserved C terminus and a variable N-terminal region, with previous reports suggesting differences between the two SEC24 subgroups in their affinity for cargo-sorting signals (18, 19). All four *Sec24* paralogs appear to be ubiquitously expressed in the adult and in the developing mouse (20, 21).

* This work was supported, in whole or in part, by National Institutes of Health Grants PO1HL057346 and RO1HL039693.
[1] Supported in part by National Institutes of Health Cellular and Molecular Biology Training Grant T32-GM007315.
[2] Investigator of the Howard Hughes Medical Institute. To whom correspondence should be addressed: Depts. of Internal Medicine and Human Genetics, Howard Hughes Medical Institute, Life Sciences Institute, University of Michigan, 210 Washtenaw Ave., Ann Arbor, MI. Tel.: 734-647-4808; Fax: 734-936-2888; E-mail: ginsburg@umich.edu.
[3] The abbreviations used are: ER, endoplasmic reticulum; HFD, high fat diet; SERT, serotonin transporter.

Mutations in several *Sec24* paralogs in zebrafish suggest a critical role in the secretion of extracellular matrix collagens (22–24). Although there have been no diseases attributed to mutations in any of the human *SEC24* paralogs, mutations in *SEC23A* result in the human disorder cranio-lenticulo-sutral dysplasia (25), and mutations in human *SEC23B* cause congenital dyserythropoietic anemia type II (26). In contrast to humans, *Sec23*-deficient mice exhibit perinatal lethality due to pancreatic destruction (27). Mice deficient in SEC24A exhibit low plasma cholesterol levels, attributed to a reduction in secretion of the regulatory protein PCSK9 (28). SEC24B-deficient mice have a specific block in the secretion of VANGL2, leading to a neural tube closure defect (29). SEC24D-deficient mice die very early in embryonic development (before E3.5) (20). We now report that the loss of murine SEC24C also results in embryonic lethality, although at a later time point (~E7 to E8). However, ablation of SEC24C in multiple tissues is surprisingly well tolerated.

EXPERIMENTAL PROCEDURES

Generation of SEC24C-deficient Mice—ES cell clone EPD0241-2-A11 was obtained from the European Mouse Mutagenesis program (EUCOMM). This clone is heterozygous for the allele $Sec24c^{tm1a(EUCOMM)Wtsi}$, a *Sec24c* allele with conditional potential, which will be referred to as $Sec24c^{GT}$. ES cells were cultured and expanded for microinjection and genomic DNA isolation as described previously (30). ES cell mouse chimeras were generated as described (31) and subsequently bred to B6(Cg)-Tyr^{c-2J}/J (JAX stock 000058) to achieve germ line transmission. ES cell-derived F1 black progeny were genotyped using primers to detect the presence ($Sec24c^{GT}$) or absence ($Sec24c^{WT}$) of the targeted allele (primers Ex and E). All primers used in this study are listed in Table 1. The $Sec24c^{GT}$ allele was maintained by continuous backcrosses to C57BL/6J mice. Genotyping was performed with mouse tail clip DNA using Go-Taq Green Master Mix (Promega, Madison, WI), and the resulting PCR products were resolved by 2% agarose gel electrophoresis.

Long Range PCR to Confirm the Insertion Site of the Sec24c Gene Trap Allele—Genomic DNA isolated from the ES cell clone EPD0241-2-A11 and genomic DNA from a wild type C57BL/6J mouse tail clip were amplified by long range PCR to confirm correct targeting of the $Sec24c^{GT}$ allele with primers GF3 and primer B (5′ end) and GR4 and primer G (3′ end) using Phusion Hot Start II DNA Polymerase (Thermo Scientific), with products resolved on a 0.8% agarose gel.

Generation of a Sec24c Conditional Allele—To generate mice carrying the conditional $Sec24c^{tm1c(EUCOMM)Wtsi}$ allele (referred to here as $Sec24c^{FL}$ allele), $Sec24c^{+/GT}$ mice were crossed to mice transgenic for Flpe recombinase driven by an actin promoter (C57BL/6J background, JAX 005703). Mice were genotyped with primers Ex and E to detect both the wild type (308 bp) allele and the presence of the LoxP site (278 bp), primers A, B, and C to distinguish between the $Sec24c^{GT}$ (204 bp) and $Sec24c^{FL}$ (534 bp) alleles, and with primers FLP1 and FLP2 to detect the FLPE transgene (750 bp). $Sec24c^{+/FL}$ mice were backcrossed to C57BL/6J mice to remove the FLPe transgene.

Generation of a Sec24c Null Allele—$Sec24c^{+/FL}$ mice were crossed to EIIA-driven Cre recombinase transgenic mice (C57/BL6 background, JAX 003724), and offspring were genotyped with primers A, Ex, and E to distinguish the $Sec24c^{+}$, $Sec24c^{FL}$, and $Sec24c^{tm1d(EUCOMM)Wtsi}$ (referred to as the $Sec24c^{-}$) alleles. The Cre transgene was detected with primers Cre-fwd and Cre-rev. $Sec24c^{+/-}$ mice were backcrossed to C57BL/6J mice to remove the Cre transgene.

Generation of Tissue-specific Knock-out Mice—$Sec24c^{FL/FL}$ mice were crossed to $Sec24c^{+/-}Cre^{+}$ using the following tissue-specific transgenes: P48-Cre (pancreas-specific, a generous gift from Christopher V. E. Wright (32)), villin-Cre (intestinal-epithelial specific, JAX 004586) (33), albumin-Cre (liver hepatocyte-specific, JAX 003574) (34), SM22-Cre mice (smooth muscle-specific, JAX 004746) (35), and Meox2-Cre transgene (ubiquitous expression beginning at embryonic day 5, JAX 003755) (36). Progeny were genotyped at the *Sec24c* locus with primers A, Ex, and E and with primers Cre-fwd and Cre-rev to detect the presence of the Cre transgene. The level of Cre-mediated excision was assessed by isolation of genomic DNA from tissue samples of either $Sec24c^{+/FL}$ Cre^{+} or $Sec24c^{FL/-}$ Cre^{+} mice and PCR using primers A, Ex, and E (Table 1) at the *Sec24c* locus.

Phenotypic Analysis of $Sec24c^{+/-}$, $Sec24c^{+/-}$, $Sec24d^{+/GT}$, and Tissue-specific Knock-out Mice—Whole blood was collected, and complete blood counts were carried out as described previously (20). For histology, tissues were fixed in 4% paraformaldehyde in PBS overnight at 4 °C and then transferred to 30% EtOH, 50% EtOH, and 70% EtOH, three times each for 10 min. Processing, embedding, sectioning, and H&E staining were performed at the Microscopy and Image Analysis Laboratory, University of Michigan. Body weights were measured weekly from weaning up to 12 weeks of age. A high fat diet (45% of calories from fat) was purchased from Research Diets (New Brunswick, NJ), and animals were fed *ad libitum*. For insulin and blood lipid analysis, mice were fasted 16 h before blood collection. Blood was collected using heparin-coated collection tubes (Fisher) by retro-orbital bleeding from mice anesthetized with isoflurane. Plasma samples were then collected by centrifugation of heparinized blood samples at 3000 × *g* for 5 min at 4 °C. Plasma cholesterol and triglyceride levels were measured in 5 μl of plasma samples with colorimetric assays using the LiquiColor cholesterol test kit (Stanbio, Boerne, TX) or serum triglyceride determination kit (Sigma) according to the manufacturer's instructions. Insulin levels were measured using the ultrasensitive mouse insulin ELISA kit (Crystal Chem, Downers Grove, IL), per manufacturer's instructions.

Timed Matings—Timed matings were carried out by intercrossing $Sec24c^{+/-}$ mice. Embryos were harvested at multiple time points, including day E7.5–11.5 for genotyping and histological analysis. Genotyping was performed on genomic DNA isolated from embryonic yolk sacs. Blastocyst collection and genotyping were performed as described previously (37) using super-ovulated $Sec24c^{+/-}$ females and $Sec24c^{+/-}$ males.

Construction of Sec24c and Sec24d Transgenes and Generation of Transgenic Mice—Transgenes carrying either *Sec24c* or *Sec24d* were designed using the previously reported pCAG3Z

TABLE 1
List of primers used in this study
All sequences are listed 5′ to 3′.

Primer name	Sequence (5′ to 3′)
Genotyping and LR-PCR primers	
A	AAGGCGCATAACGATACCA
B	CACAACGGGTTCTTCTGTTAGTCCC
C	CTTGAGGCAAGAATGCAAAACAAGAATC
Ex	GTACTAGGTGAGCCTGAAATCAATG
E	ACTAAGATGGGTCCACAAAAGAGC
FLP1	GGTCCAACTGCAGCCCAAGCTTCC
FLP2	GTGGATCGATCCTACCCCTTGCG
Cre-fwd	TTACCGGTCGATGCAACGAGT
Cre-rev	TTCCATCAGTGAACGAACCTGG
GF3	GCTGATACTGATACTAGGATCCACGGACAG
GR4	GCACTGCTAACAGTTCGCTATTCCTTCCG
G	CACACCTCCCCCTGAACCTGAAAC
Tg-F	AAATCTGTGCGGAGCCGAAATCTG
Tg-R	GCATGAACATGGTTAGCAGAGGCT
RT-PCR primers	
GAPDH-fwd	TGTGATGGGTGTGAACCACGAGAA
GAPDH-rev	ACCAGTGGATGCAGGGATGATGTT
24c-F	GTGTGACCGGCGGCTCTA
24c-R	GGGGCTGCAGGTCCTGGTTG
24d-F	TTGGCAAAGAATTCCTCGACCTG
24d-R	ATCTTTGAGGAGGATGGCCTGGA
Primer V	GCCCTCAACCTAATTATGAGAGCCCA
Primer W	CCCGTACACCAGTAACAAATGGCT
Primer X	TCTCAGCAGTTTGGTCCTCCATTG
Primer Y	TTTGCTGCAGCTGATAACCAGG
Primers for transgene construction	
P1	GAATACTCAAGCTTGCATGCCTGCAGGTCG
P2	AGAGCATGCATGAGATCACCGGTCATCACCGT GGCGGCCGCTCATAATCAGCCATAC
P3	ACGTACACCGGTGCTCTCATAATGAATG
P4	CTAGTCTGCGGCCGCTTAGCTCAGTAGCTG CCGGATC
P5	ACGTACACCGGTATTTTCATCATGAGCC
P6	TCGCTAGGCGGCCGCTCAGTTAAGCAGTTG

vector (38). The CAG promoter contains the CMV intermediate-early enhancer and the chicken β-actin promoter to drive early, ubiquitous expression (39, 40) of either *Sec24c* or *Sec24d*. AgeI and NotI sites were added upstream of an SV40 early termination signal and a poly(A) signal isolated from Tg2.33 (38), and this was placed downstream of the CAG promoter in the pCAG3Z vector to create pCAG3zS. *Sec24c* (cDNA −9 to 3290) or *Sec24d* (cDNA −9 to 3098) was inserted between the CAG promoter and the SV40 signal using AgeI and NotI. DNA sequencing was performed on all constructs prior to microinjection to verify the integrity of the transgenes. All primers used to create these constructs (P1–P6) are listed in Table 1. pCAG3zS-Sec24c and pCAGzS-Sec24d were liberated from the vector backbone with a double digest with BamHI-HF/SphI-HF or SacI/HindIII, respectively (New England Biolabs), and transgenic mice were generated by the University of Michigan Transgenic Animal Model Core as described previously (41). Transgenic founders (C57BL/6J × SJL F2) for both lines were detected by PCR using Tg-F and Tg-R located in the promoter region of the transgenes. Mice transgenic for either pCAG3zS-Sec24c or pCAG3zS-Sec24d were crossed with $Sec24c^{+/-}$ mice to generate $Sec24c^{+/-}$ Tg^{+} mice, which were then crossed to $Sec24c^{+/-}$ mice to generate potential $Sec24c^{-/-}$ Tg^{+} mice. All progeny were genotyped at the *Sec24c* locus and for the presence of the transgene. Similar crosses were also performed with $Sec24d^{+/GT}$ (20) mice. Five founders for pCAG3zS-Sec24c were used to generate transgenic lines to test the ability of pCAG3zS-Sec24c to rescue the loss of *Sec24c*. Four pCAG3zS-Sec24d founders were used to generate transgenic lines.

Reverse Transcription-PCR—Total RNA was isolated from a panel of frozen tissues from transgenic mice from each of the founder lines using an RNeasy kit (Qiagen) as per manufacturers instructions. cDNA synthesis and PCR were carried out in one reaction using SuperScript® III one-step RT-PCR system with Platinum®Taq (Invitrogen) per manufacturer's instructions. Primers V, W, X, and located in *Sec24c* exons 4–7 were used to amplify signal from *Sec24c* cDNA. Primers 24c-F or 24d-F and primers 24c-R or 24d-R were used to detect cDNA specific for the *Sec24c* or *Sec24d* transgenes. GAPDH amplification with primers GAPDH-fwd and GAPDH-rev was carried out in parallel for each sample.

Statistical Analysis—*p* value for progeny genotypes were calculated by a χ^2 test comparing the expected ratio of genotypes to those observed. For intercrosses of $Sec24c^{+/GT}$, $Sec24c^{+/FL}$, or $Sec24c^{+/-}$ mice, the expected ratio of homozygous mice to all other expected genotypes (25:75) was used. Complete blood count parameters were evaluated for significance using Student's *t* test. The α levels were adjusted for multiple observations according to the Bonferroni correction.

RESULTS

Sec24c mRNA expression was detected by RT-PCR in all 15 adult mouse tissues tested, consistent with previously reported human expression patterns (16, 42). RT-PCR analysis also detected an alternative in-frame exon (exon 6*, encoding 23 amino acids), present in a subset of *Sec24c* mRNAs (Fig. 1). The transcript containing this additional exon (*Sec24c-2*) was detected only in brown adipose tissue, skeletal muscle, brain (Fig. 1*C*), and the heart, with only low levels of the transcript skipping exon 6* (*Sec24c-1*) detected in these tissues (Fig. 1*C*). *Sec24c-1* is the only splice form detected in lung, kidney, stomach, large intestine, and small intestine (Fig. 1*C*) as well as the adrenal gland, liver, salivary gland, testis, spleen, and white adipose tissue (data not shown).

Correct targeting of the $Sec24c^{GT}$ allele (Fig. 2*A*) was confirmed by long range PCR (Fig. 2*B*), with PCR genotyping primers (A, Ex, and E) differentiating between each *Sec24c* allele used in this study (Fig. 2*C*). Genotypes of 2-week-old progeny from $Sec24c^{+/GT}$ intercrosses revealed the expected number of wild type and heterozygous offspring but none of the expected ¼ $Sec24c^{GT/GT}$ mice ($p < 2.3 \times 10^{-6}$, Table 2A). Intercrosses of $Sec24c^{+/FL}$ (obtained by excision of the β-geo cassette from $Sec24c^{GT}$, Fig. 2*A*) generated the expected number of $Sec24c^{FL/FL}$ mice (Table 2B) demonstrating that loss of $Sec24c^{GT/GT}$ mice results from the presence of the gene trap cassette, rather than a passenger gene effect (43). EIIA-Cre-mediated excision of $Sec24c^{FL}$ generated the $Sec24c^{-}$ allele (Fig. 2*A*), which lacks exon 3 and results in a frameshift and early termination codon. Intercrosses of $Sec24c^{+/-}$ mice confirm uniform loss of $Sec24c^{-/-}$ mice by 2 weeks of age (Table 2C). At embryonic day 10.5–11, no intact $Sec24c^{-/-}$ embryos were observed. However, empty yolk sacs were present and could be separated from maternal tissue, with genotyping identifying the missing embryos as $Sec24c^{-/-}$. Genotypes were also assessed at E9.5;

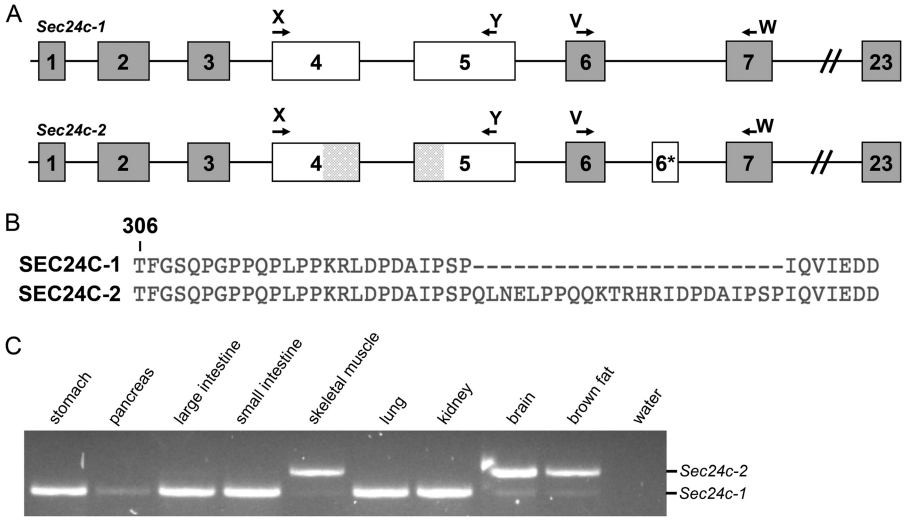

FIGURE 1. **Identification of an alternative splice form of *Sec24c*.** *A,* schematic of the two *Sec24c* splice forms observed in mice. *Arrows* indicate primers used to detect the presence of the alternative exon (6*). *Shaded regions* in exons 4 and 5 represent exonic sequence present in *Sec24c-2* that is absent from another RefSeq splice variant annotated as containing exon 6* (NM_001168273.1), which was not detected in our RT-PCR. *B,* protein sequence alignment beginning at Thr-306 of SEC24C-1 and SEC24C-2 showing the additional 23 amino acids encoded by exon 6*. *C,* RT-PCR using primers V and W, which detects a 249-bp product from *Sec24c-2* and a 180-bp product from *Sec24c-1*.

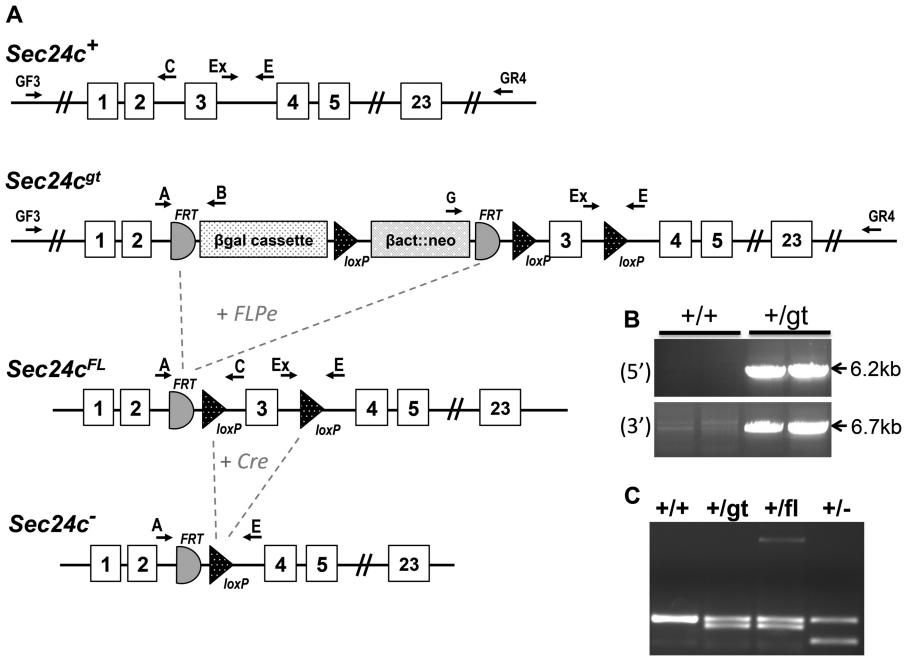

FIGURE 2. **Generation of *Sec24c* conditional and null alleles.** *A,* schematic of the original *Sec24c*^{GT} allele. FLPe-mediated excision yields the conditional *Sec24c*^{FL} allele, and subsequent Cre-mediated excision gives rise to the null *Sec24c*$^{-}$ allele. Primers used for genotyping are indicated. *B,* long range PCR confirms correct targeting for the original *Sec24c*^{GT} allele. Primers GF3 and GR4 are located outside of the homology arms. Primers GF3 and B amplify a 6234-bp product from the 5′ end of the *Sec24c*^{GT} allele, and primers G and GR4 amplify a 6648-bp product from the 3′ end. As expected, neither set of primers yields a product from the *Sec24c*^{WT} allele. *C,* genotyping with primers A, Ex, and E distinguishes between the wild type (308 bp), gene trap or floxed (278 bp), and null alleles (225 bp).

again, for null embryos, only empty yolk sacs were detected, although at E8.5, one *Sec24c*$^{-/-}$ embryo appeared to have been dead for ~12 h (blinded observation prior to genotyping). Histological analysis of E7.5 embryos and decidual swellings from a *Sec24c*$^{+/-}$ intercross revealed a series of morphologies ranging in severity from embryos that appeared to be gastrulating and developing normally (Fig. 3, *A, B,* and *D*), those that had not yet begun gastrulation and exhibited a thinned embryonic ectoderm (Fig. 3*C*), those in which the embryonic ectoderm was disorganized (Fig. 3*E*), and implantation sites containing remnants of the egg cylinder and membranes (Fig. 3*F*). Although no genotypes were assigned to the sectioned implantation sites (Fig. 3, *D–F*), *Sec24c*$^{+/+}$ (Fig. 3*A*) and *Sec24c*$^{+/-}$ (Fig. 3*B*) embryos appear to develop normally, in contrast to the *Sec24c*$^{-/-}$ embryo depicted in Fig. 3*C*. Taken together, these data suggest that SEC24C deficiency is lethal between E7.0 and E8.5. Although the cause of death remains unknown, it appears that SEC24C is required in the embryonic ectoderm just prior to gastrulation. Analysis of progeny from *Sec24c*$^{+/-}$ intercrosses and backcrosses to wild type mice indicates that

TABLE 2

Sec24c allelic series genotype distributions

A, results of $Sec24c^{+/GT}$ intercrosses and backcrosses are shown. B, results of $Sec24c^{+/FL}$ intercrosses are shown. C, results of $Sec24c^{+/-}$ intercrosses and backcrosses are shown.

A. Genotype:	$Sec24c^{+/+}$	$Sec24c^{+/GT}$	$Sec24c^{GT/GT}$	*p*-value
$Sec24c^{+/GT}$ x $Sec24c^{+/GT}$ expected:	25%	50%	25%	
2-weeks of age (n=67)	36% (24)	64% (43)	0%	$p < 2.3\text{x}10^{-6}$
$Sec24c^{+/GT}$ x $Sec24c^{+/+}$ expected:	50%	50%	--	
2 weeks of age (n=100)	53% (53)	47% (47)	--	$p > 0.54$
B. Genotype:	$Sec24c^{+/+}$	$Sec24c^{+/FL}$	$Sec24c^{FL/FL}$	*p*-value
$Sec24c^{+/FL}$ x $Sec24c^{+/FL}$ expected:	25%	50%	25%	
2-weeks of age (n= 102)	26% (26)	42% (43)	32% (33)	$p > 0.08$
C. Genotype:	$Sec24c^{+/+}$	$Sec24c^{+/-}$	$Sec24c^{-/-}$	*p*-value
$Sec24c^{+/-}$ x $Sec24c^{+/-}$ expected:	25%	50%	25%	
2-weeks of age (n=184)	40% (73)	60% (111)	0%	$p < 4.9\text{x}10^{-15}$
E10.5-E11 (n=26)	12% (3)	73% (19)	15% (4*)	$p > 0.17$
E9.5 (n=21)	38% (8)	48% (10)	14% (3*)	$p > 0.25$
E8.5 (n=7)	29% (2)	57% (4)	14% (1**)	$p > 0.51$
E7.5 (n=22)	23% (5)	59% (13)	18% (4)	$p > 0.46$
Blastocyst (n=47)	30% (14)	40% (19)	30% (14)	$p > 0.42$
Total (n=307)	**34% (105)**	**57% (176)**	**9% (26)**	$p < 2.2\text{x}10^{-11}$
$Sec24c^{+/-}$ x $Sec24c^{+/+}$ expected:	50%	50%	--	
2 weeks of age (n=146)	57% (83)	43% (63)	--	$p > 0.09$

* All $Sec24c^{-/-}$ embryos from E9.5 to E11 were absent, but yolk sacs were able to be isolated for genotyping.

** Embryo was noted to have been dead for ~12 h. All embryonic observations were made prior to genotyping analysis.

heterozygous mice are present in the expected ratios (Table 2C).

As noted above, the expected numbers of $Sec24c^{+/GT}$ and $Sec24c^{+/-}$ mice are observed at 2 weeks of age. Growth and complete blood counts of heterozygous mice were also indistinguishable from their wild type littermates (Fig. 4 and Table 3). Adult $Sec24c^{+/-}$ mice are fertile and exhibit no gross or microscopic abnormalities on standard autopsy examination (Fig. 4C). Although only a small number of wild type littermates were followed beyond 100 days, no significant difference was observed in the life span of $Sec24c^{+/-}$ mice ($n = 21$) compared with controls.

To test the potential overlap in function between SEC24C and SEC24D (16), we performed intercrosses between $Sec24c^{+/-}$ and $Sec24d^{+/GT}$ mice (Table 4) (20). At 2 weeks of age, double heterozygous mice are present at the expected Mendelian ratio ($p > 0.12$). No differences were observed in growth to 12 weeks (Fig. 5, *A* and *B*) or complete blood count analyses (Table 3), when compared with WT or single heterozygous littermates. Although only a small number of wild type littermates were followed beyond 100 days, no significant difference was observed in the life span of $Sec24c^{+/-}$ $Sec24d^{+/GT}$ mice ($n = 27$) compared with controls. Routine autopsy and histological survey were also unremarkable (Fig. 5C).

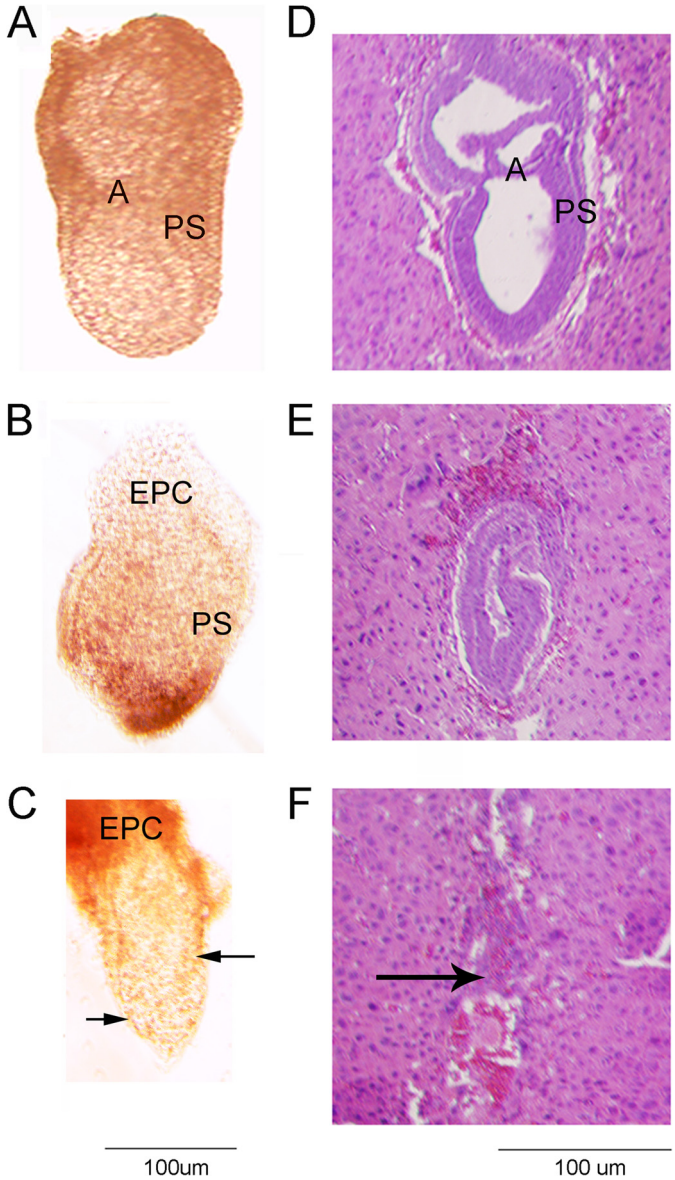

FIGURE 3. **Phase contrast (*A–C*) and H&E staining (*D–F*) of E7.5 embryos resulting from $Sec24c^{+/-}$ intercrosses.** E7.5 embryos were removed from the decidua and photographed prior to fixation (*A–C*), or whole decidual swellings were fixed and sectioned (*D–F*). Images are representative of the types of embryonic development/loss observed in 22 embryos. *A, B,* and *D* illustrate normal gastrulation. Genotypes were obtained for *A–C* (*A*, $Sec24c^{+/+}$; *B*, $Sec24c^{+/-}$; *C*, $Sec24c^{-/-}$). The embryo in *C* exhibits thinning of the embryonic ectoderm. *E* illustrates a disorganized embryo, and *F* shows remnants of the egg cylinder. Anterior is to the *left* of each embryo; *A* = amniotic fold; *EPC* = ectoplacental cone; *PS* = primitive streak. *Arrow* in *F* indicates remnants of the embryo.

Transgenes designed to express SEC24C or SEC24D from the ubiquitous chick β-actin promoter (Fig. 6*A*) were generated and tested for their ability to rescue the lethal $Sec24c^{-/-}$ phenotype. No $Sec24c^{-/-}$ Tg^{+} mice survived to weaning for either the SEC24C (1 line, $n = 34$) or SEC24D (1 line, $n = 49$) transgene. Similarly, crosses to the $Sec24d^{GT}$ mice failed to demonstrate rescue of the $Sec24d^{GT/GT}$ lethal phenotype by either transgene; for the SEC24D transgene, no rescues were observed out of 149 transgenic mice from five different founder lines, with *n* for each line ranging from 9 to 43 transgenic progeny. For the SEC24C transgene, no rescues were observed out of 130

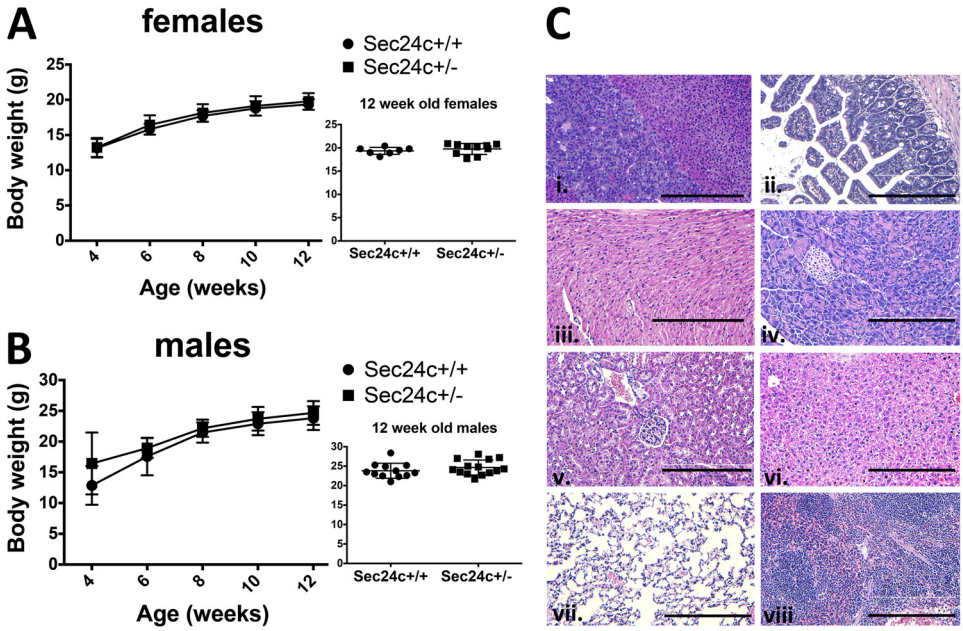

FIGURE 4. ***Sec24c*$^{+/-}$ mice are phenotypically normal.** Growth curves of female (*A*) and male (*B*) mice indicate no difference in body weights between heterozygous mice and wild type littermate controls, with $p > 0.05$ at all time points. *Error bars* represent standard deviation. *C,* H&E staining of *Sec24c*$^{+/-}$ tissues reveals no abnormalities in a panel of tissues, including adrenal gland (*panel i*), intestine (*panel ii*), heart (*panel iii*), pancreas (*panel iv*), kidney (*panel v*), liver (*panel vi*), lung (*panel vii*), and spleen (*panel viii*). *Scale bar,* 0.25 μm.

TABLE 3

Complete blood count analysis of mice from *Sec24c*$^{+/-}$ × *Sec24d*$^{+GT}$ intercrosses

Tail bleeds were carried out at 8–12 weeks of age. Data from males and females were pooled after confirming no significant difference between males and females of the same genotypes. The following abbreviations are used: HGB, hemoglobin; HCT, hematocrit; MCV, mean corpuscular volume; MCH, mean corpuscular hemoglobin; MCHC, MCH concentration; RDW, red cell distribution width; PLT, platelet count; MPV, mean platelet volume.

Parameter	Genotype			
	Sec24c$^{+/+}$	*Sec24c*$^{+/-}$	*Sec24d*$^{+/GT}$	*Sec24c*$^{+/-}$ *Sec24d*$^{+/GT}$
WBC (× 10^3 cells/μl)	7.4 ± 0.9	8.2 ± 1.3	9.9 ± 1.4	9.0 ± 1.1
RBC (× 10^6 cells/μl)	8.7 ± 0.8	9.5 ± 0.3	9.7 ± 0.2	9.9 ± 0.3
HGB (g/dl)	12.2 ± 1.0	12.2 ± 0.5	13.3 ± 0.2	13.0 ± 0.5
HCT (%)	45.2 ± 2.6	45.7 ± 1.5	48.5 ± 0.7	48.4 ± 1.3
MCV (fl)	48.8 ± 0.6	48.1 ± 0.5	49.8 ± 0.4	49.1 ± 0.4
MCH (pg)	13.1 ± 0.3	12.6 ± 0.2	13.6 ± 0.1	13.1 ± 0.1
MCHC (g/dl)	26.9 ± 0.7	26.3 ± 0.5	27.2 ± 0.4	26.8 ± 0.4
RDW (%)	13.5 ± 0.3	13.5 ± 0.2	13.9 ± 0.5	14.0 ± 0.6
PLT (× 10^3 cells/μl)	976.0 ± 171.7	1221.7 ± 53.3	1186.7 ± 80.9	1076.3 ± 73.0
MPV (fl)	5.3 ± 0.6	5.0 ± 0.2	4.8 ± 0.2	5.1 ± 0.2

TABLE 4

Results of *Sec24c*$^{+/-}$ *Sec24d*$^{+/GT}$ intercross

Mice are genotyped at 2 weeks of age. *Sec24d*$^{+/GT}$ mice are on C57BL/6J background (>*n*18).

Genotype	*Sec24c*$^{+/+}$ *Sec24d*$^{+/+}$	*Sec24c*$^{+/-}$ *Sec24d*$^{+/+}$	*Sec24c*$^{+/+}$ *Sec24d*$^{+/GT}$	*Sec24c*$^{+/-}$ *Sec24d*$^{+/GT}$	*p* value
Expected ratio of F1 progeny	25%	25%	25%	25%	
Observed F1 progeny (n = 94)	32% (30)	26% (24)	24% (23)	18% (17)	$p > 0.12$

transgenic mice from four founder lines, with *n* for each line ranging from 11 to 57 transgenic progeny. RT-PCR analysis indicates that mRNA from the transgenes is being expressed in all tissues tested (Fig. 6*B*).

To test the requirement for SEC24C in specific adult tissues, *Sec24c*$^{FL/FL}$ mice were crossed with mice carrying Cre transgenes specific for the pancreas (p48-Cre), hepatocytes (albumin-Cre), smooth muscle cells (SM22-Cre), and intestinal epithelial cells (villin-Cre) (Table 5). *Sec24c*$^{FL/-}$ *Cre*$^{+}$ mice were observed in the expected numbers for p48-Cre ($p > 0.65$), SM22-Cre ($p > 0.46$), villin-Cre ($p > 0.46$), and albumin-Cre ($p > 0.10$). Although Cre-mediated excision of the *Sec24c*^{FL} allele was nearly complete in the pancreas of p48Cre^{+} mice (Fig. 7*A*), pancreatic acinar and islets appear entirely normal by routine histology (Fig. 7*B*). *Sec24c*$^{FL/-}$*p48-Cre*$^{+}$ also exhibit normal weight gain through 12 weeks of age compared with their littermate controls on either normal chow (Fig. 8, *A* and *B*) or high fat diet (HFD) (Fig. 9, *A* and *B*). Similar results were observed for the albumin-Cre and villin-Cre transgenes, although the levels of excision were not as complete in these tissues as in the pancreas of p48-Cre^{+} mice (Fig. 7). There were also no differences in plasma cholesterol or triglyceride levels in tissue-specific knockouts *versus* littermate controls on HFD for p48-Cre, albumin-Cre, and villin-Cre transgenes (Figs. 9–11), and insulin levels between *Sec24c*$^{FL/-}$*p48-Cre*$^{+}$ and corresponding littermate controls on HFD were also indistinguish-

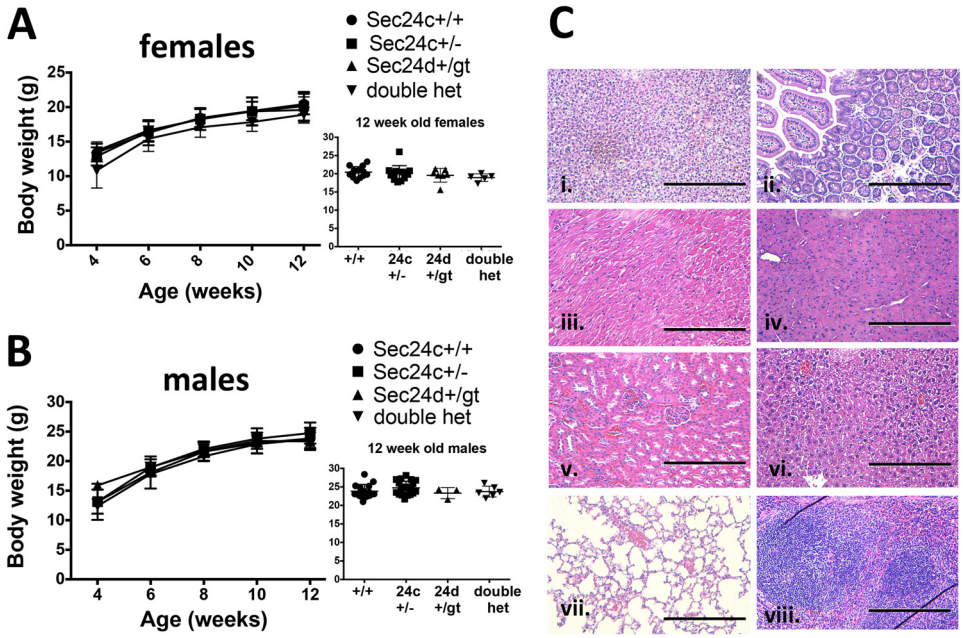

FIGURE 5. ***Sec24c*$^{+/-}$ *Sec24d*$^{+/GT}$ mice are phenotypically normal.** Growth curves of female (*A*) and male (*B*) mice indicate no difference in body weights between heterozygous mice and littermate controls, with $p > 0.05$ at all time points. *Error bars* represent standard deviation. "*Double het*" = *Sec24c*$^{+/-}$ *Sec24d*$^{+/GT}$. *C*, H&E staining of *Sec24c*$^{+/-}$ *Sec24d*$^{+/GT}$ tissues does not reveal any abnormalities in a panel of tissues, including adrenal gland (*panel i*), intestine (*panel ii*), heart (*panel iii*), pancreas (*panel iv*), kidney (*panel v*), liver (*panel vi*), lung (*panel vii*), and spleen (*panel viii*). *Scale bar*, 0.25 μm.

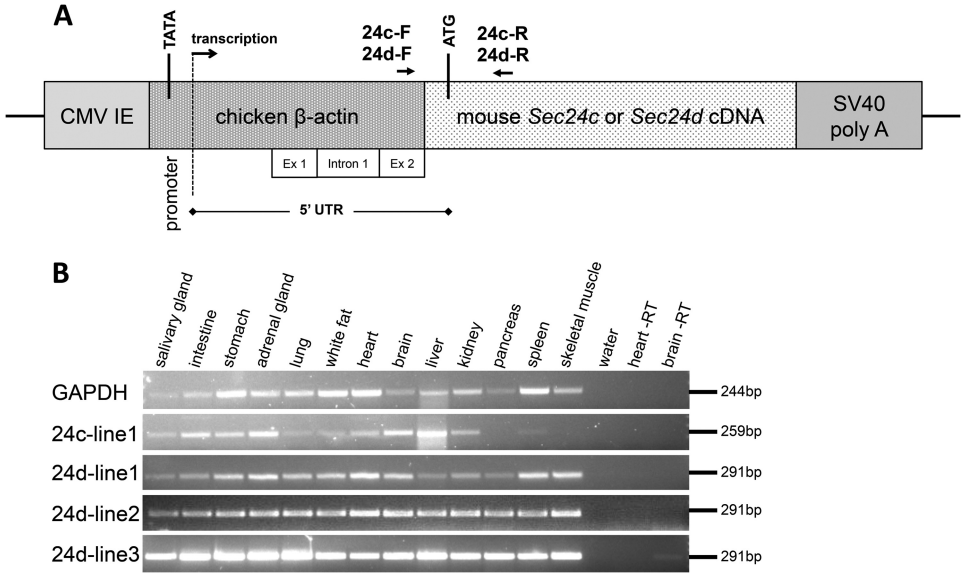

FIGURE 6. **Ubiquitous transgenic expression of *Sec24c* and *Sec24d*.** *A*, diagram of the pCAG3zS-Sec24c or -Sec24d transgenic construct, adapted from Ref. 38, including transcription start site, initial ATG, and polyadenylation signal. *CMV IE* = cytomegalovirus immediate-early enhancer; *UTR* = untranslated region; *SV40 poly(A)* = simian virus 40 polyadenylation signal. Primers 24c-F, 24c-R, 24d-F, and 24d-R were used for RT-PCR of transgenes expressing *Sec24c* or *Sec24d*, respectively. *B*, transgene expression in a panel of tissues for founder lines 24c-line1, 24d-line1, 24d-line2, and 24d-line3. Heart and brain RT samples were carried out in the absence of reverse transcriptase.

TABLE 5

Results of tissue-specific deletion of *Sec24c*

Mice are genotyped at 2 weeks of age. p48-Cre = pancreatic cells; SM22-Cre = smooth muscle cells; villin-Cre = intestinal epithelial cells; albumin-Cre = liver hepatocytes; Meox2-Cre = ubiquitous Cre expressed beginning around embryonic day 5.

Genotype	*Sec24c*$^{+/FL}$	*Sec24c*$^{+/FL}$ *Cre*$^{+}$	*Sec24c*$^{FL/-}$	*Sec24c*$^{FL/-}$*Cre+*	*p* value
Expected ratio of test cross-progeny	25%	25%	25%	25%	
Cre line					
p48-Cre (n = 148)	20.9% (31)	25.7% (38)	27.7% (41)	25.7% (38)	$p > 0.65$
SM22-Cre (n = 40)	32.5% (13)	15.0% (58)	22.5% (9)	30% (12)	$p > 0.46$
Villin-Cre (n = 143)	28.7% (41)	22.4% (32)	26.5% (38)	22.4% (32)	$p > 0.46$
Albumin-Cre (n = 123)	23.6% (29)	31.7% (39)	26.0% (32)	18.7% (23)	$p > 0.10$
Meox2-Cre (n = 69)	37.7% (26)	20.3% (14)	42.0% (29)	0% (0)	$p < 1.7 \times 10^{-6}$

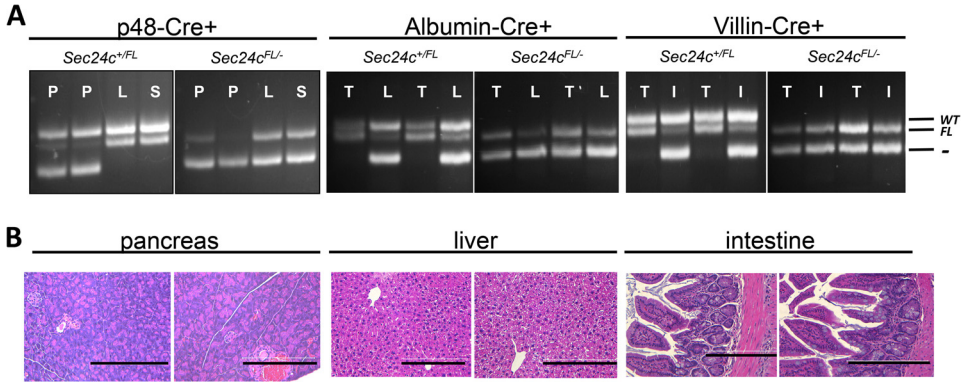

FIGURE 7. **Tissue-specific Cre-mediated excision of *Sec24c*^{FL} allele.** *A,* genotyping for Cre-mediated excision in the pancreas (*P*), liver (*L*), spleen (*S*), intestine (*I*), and tail (*T*) in *Sec24c*$^{+/FL}$ and *Sec24c*$^{FL/-}$ mice carrying the p48-Cre, albumin-Cre, or villin-Cre transgenes. The floxed allele is excised to generate the null allele in the pancreas, liver, or intestine, respectively, but is preserved in other tissues. The sizes of the expected products for wild type (*WT*), flox (*FL*), and null (−) alleles are indicated. *B,* H&E staining of pancreatic tissue from *p48-Cre*$^{+}$ mice, liver tissue from *albumin-Cre*$^{+}$ mice, and intestine from *villin-Cre*$^{+}$ mice show no abnormalities. *Scale bar,* 0.25 μm.

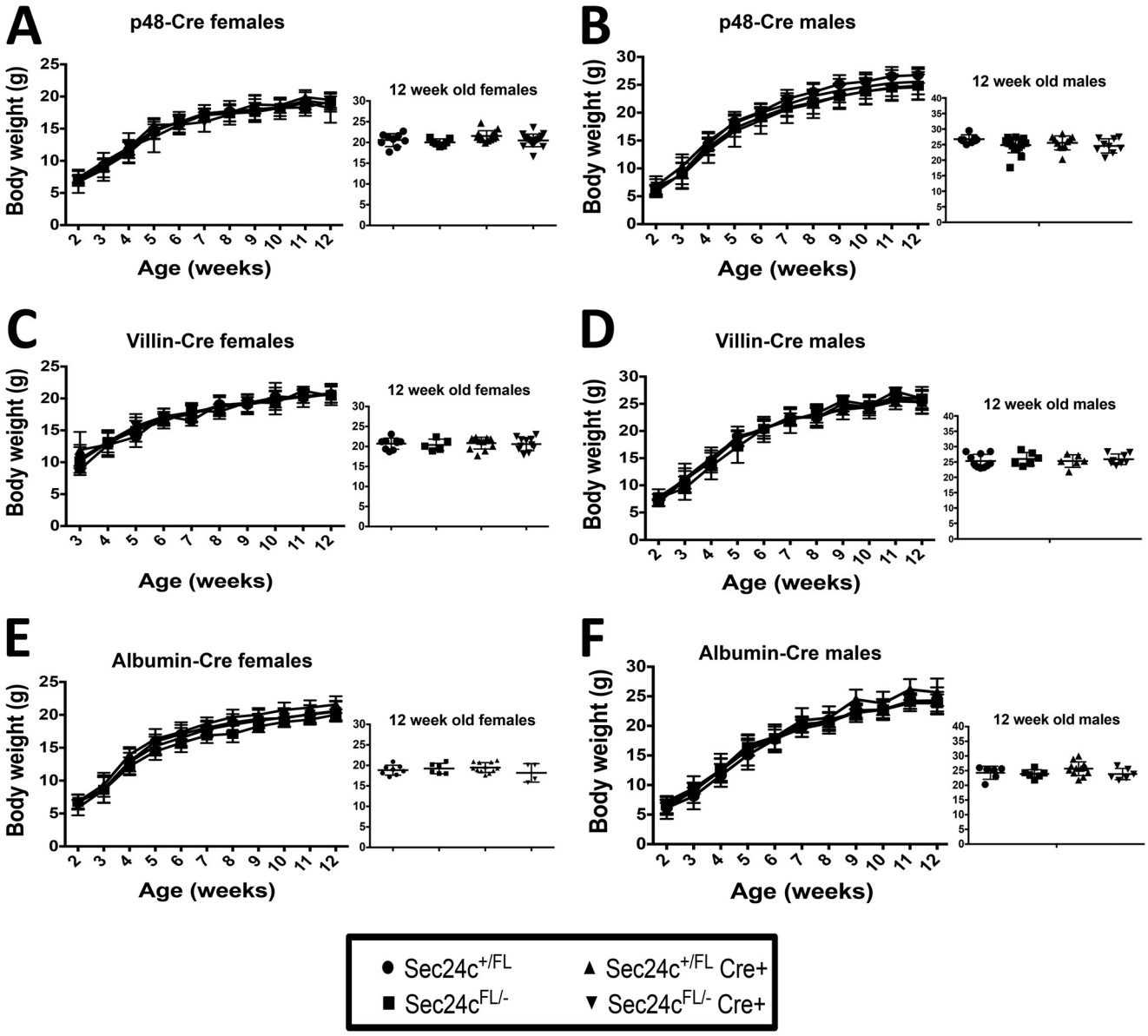

FIGURE 8. **Loss of SEC24C in the pancreas, liver, or intestine has no effect on growth.** Body weight analysis over 12 weeks of *Sec24c*$^{FL/-}$*p48-Cre*$^{+}$ mice (*A* and *B*), *Sec24c*$^{FL/-}$ *albumin-Cre*$^{+}$ mice (*C* and *D*), and *Sec24c*$^{FL/-}$*villin-Cre*$^{+}$ mice (*E* and *F*) with corresponding littermate controls in females and males. *Insets* show individual body weights at 12 weeks. $p > 0.05$ at all time points. *Error bars* represent standard deviation.

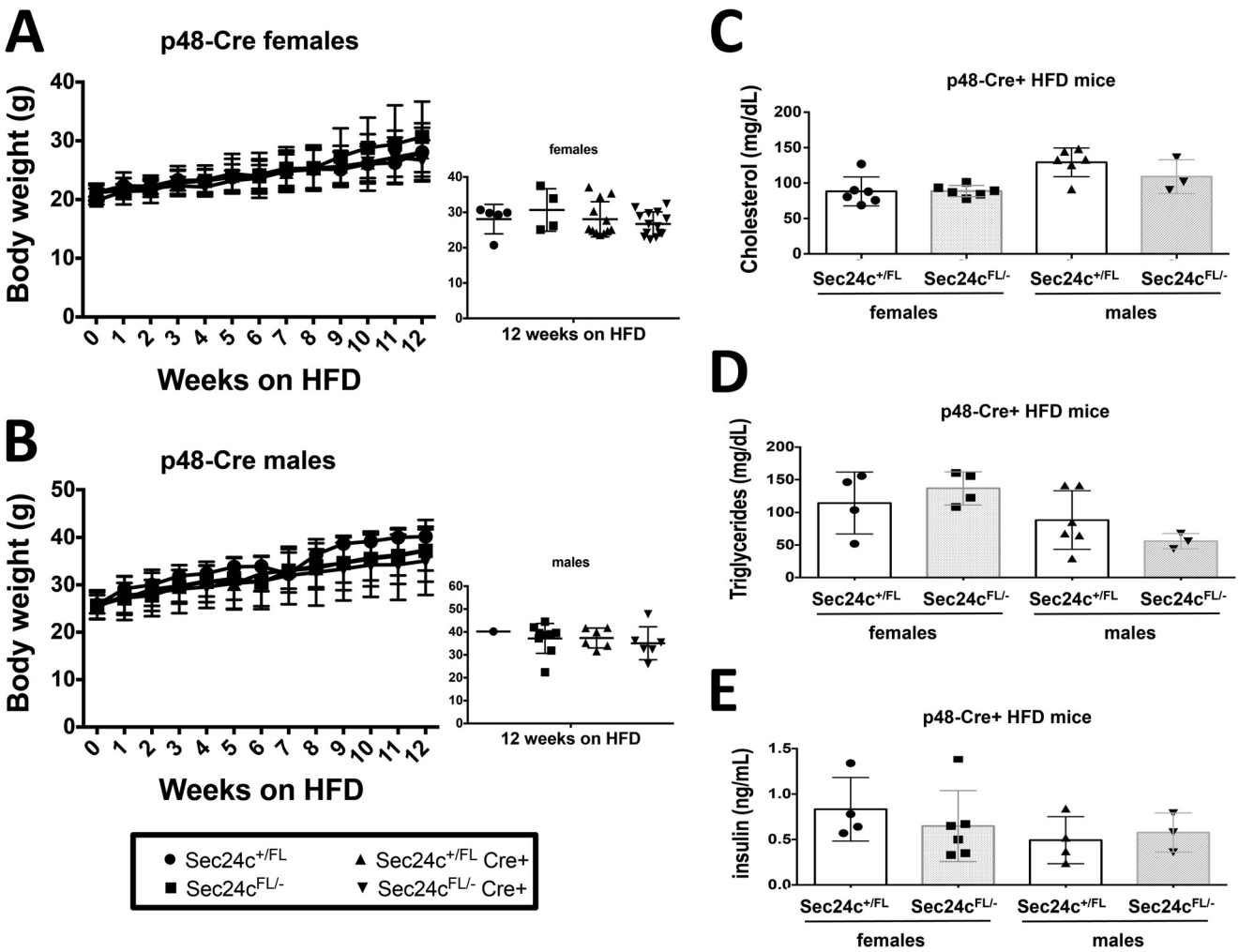

FIGURE 9. ***Sec24c$^{FL/-}$p48-Cre^{+}* mice display expected diet-induced obesity.** *Sec24c$^{FL/-}$p48-Cre^{+}* and littermate controls show no difference in weight gain over 12 weeks on HFD for females (*A*) and males (*B*), with $p > 0.05$ at all time points. Cholesterol levels (*C*), triglyceride levels (*D*), and insulin levels (*E*) are indistinguishable from littermate controls after 12 weeks on HFD. All *p* values >0.05 and *error bars* represent standard deviation.

able (Fig. 9*E*). *Sec24c$^{FL/-}$ SM22-Cre^{+}* mice exhibited no gross abnormalities and were able to carry litters to term, and although excision of *Sec24c* in smooth muscle cells in *SM22-Cre^{+}* mice was not measured directly, it is expected to be complete, based on previous reports (44). *Sec24c$^{FL/-}$ Meox2-Cre^{+}* mice were not observed at 2 weeks of age ($p < 1.7 \times 10^{-6}$, see Table 5).

DISCUSSION

Our results demonstrate that SEC24C is required for post-implantation embryonic development in the mouse, with SEC24C-deficient embryos lost in the developmental interval between implantation and E8.5. The loss of *Sec24c$^{FL/-}$ Meox2-Cre^{+}* mice is consistent with these data, as Meox2-Cre is expressed ubiquitously beginning around embryonic day 5 (36). Data from tissue-specific knockouts reveal that SEC24C is dispensable in a number of cell types, including pancreatic acinar cells (involved in the secretion of digestive enzymes), islet cells (responsible for the production and secretion of a number of hormones, including insulin), hepatocytes (the primary cell type in the liver), intestinal epithelial cells (which line the intestine), and smooth muscle cells (found in the aorta, uterus, intestine, and in vascular walls), suggesting that the three remaining *Sec24* paralogs can compensate for the loss of SEC24C in these tissues. These observations, together with the surprisingly limited but very distinct phenotypes of SEC23B (27), SEC24A (28), and SEC24B (29) deficiencies in the mouse and SAR1B (45), SEC23A (25), and SEC23B (26) deficiencies in humans, suggest at least partial overlap in function among the sets of mammalian SEC23, SEC24, and SAR1 paralogs, with unique requirements of a limited subset of cargoes likely accounting for the above phenotypes.

It has been reported that the serotonin transporter (SERT) requires SEC24C for efficient ER export (46). Given that SERT-deficient mice are viable and fertile (47), it is unlikely that the embryonic lethality observed in the SEC24C-deficient mice can be explained by defective trafficking of SERT to the plasma membrane. In addition, SERT does not become transcriptionally active until embryonic day 10 (47), well after the lethality we observed in the *Sec24c$^{-/-}$* embryos. Thus, this embryonic lethality is likely due to a trafficking defect in another as yet unidentified secretory protein(s).

The apparently normal phenotype of *Sec24c$^{+/-}$* and *Sec24c$^{+/-}$ Sec24d$^{+/GT}$* mice demonstrates a tolerance for mod-

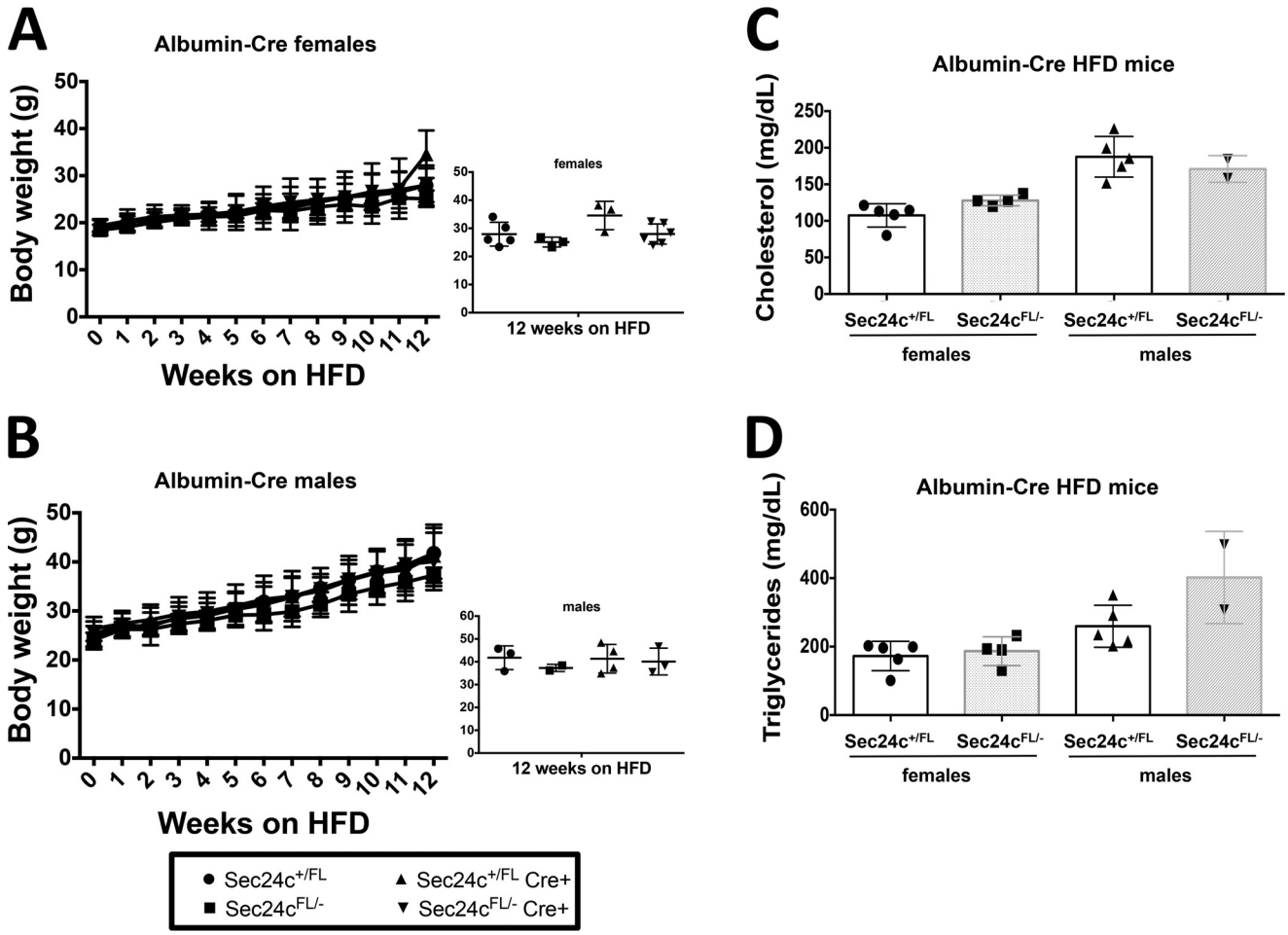

FIGURE 10. ***Sec24c*$^{FL/-}$*albumin-Cre*$^{+}$ mice display expected diet-induced obesity.** *Sec24c*$^{FL/-}$*albumin-Cre*$^{+}$ and littermate controls show no difference in weight gain over 12 weeks on HFD for females (*A*) and males (*B*), with $p > 0.05$ at all time points. Cholesterol levels (*C*) and triglyceride levels (*D*) are indistinguishable from littermate controls after 12 weeks on HFD. All *p* values >0.05 and *error bars* represent standard deviation.

erate quantitative changes in the levels of these two COPII components, consistent with previous reports of mice doubly heterozygous for *Sec24a* and *Sec24d* or *Sec24b* (28). Although an overlap in function between SEC24A and -B was observed in *Sec24a*$^{-/-}$ *Sec24b*$^{+/-}$ mice, similar experiments were precluded for SEC24C and -D, given the early embryonic lethality observed with both single homozygotes. The more severe phenotype of deficiencies in SEC24C/D compared with SEC24A/B is surprising, in light of the higher level of sequence identity between the SEC24A/B subfamily and the ancestral yeast paralog, Sec24p, and of SEC24C/D with the nonessential yeast homolog Lst1p (16). The later survival and unique phenotypes of *Sec24a*$^{-/-}$ and *Sec24b*$^{-/-}$ mice facilitated the identification of specific cargoes for each paralog (PCSK9 and VANGL2, respectively) largely explaining the observed phenotypes (28, 29). Given very early embryonic loss of mice deficient in either SEC24C or SEC24D, identification of a precise cause of death and the specific cargo(es) represents an even greater challenge. Nonetheless, our data suggest that SEC24C, like SEC24D, is required for the recruitment of critical cargo(es) at an early stage of development. The survival of SEC24C-deficient embryos well beyond the time point at which *Sec24d*$^{GT/GT}$ embryos are lost suggests a difference in SEC24C/D expression programs in early development and/or key cargo(es) uniquely dependent on SEC24D.

To date, no human disorders attributable to mutations in *SEC24C* have been identified. Analysis of data from the human Exome Variant Server (NHLBI GO Exome Sequencing Project, Seattle, WA, accessed January, 2014) identifies an allele frequency of 1% for predicted "damaging" variants in *SEC24C* in both African and European populations. This allele frequency would predict a population prevalence of 1.13×10^{-4} for individuals homozygous or compound heterozygous for damaging mutations in *SEC24C*. The absence of previous reports of human SEC24C deficiency could be due to early embryonic lethality, similar to the mouse phenotype. However, a much milder phenotype in SEC24C-deficient humans cannot be excluded. Of note, striking differences in phenotypes across species for deficiency of specific COPII paralogs have been reported previously, including very early embryonic lethality in SEC24D-deficient mice (20) compared with isolated skeletal defects in zebrafish (24) and congenital anemia in humans with mutations in *SEC23B* (26) compared with a pancreatic phenotype in mice (27).

Our analysis identified two alternatively spliced forms of mouse *Sec24c* mRNA, *Sec24c-1* (RefSeq (49) accession

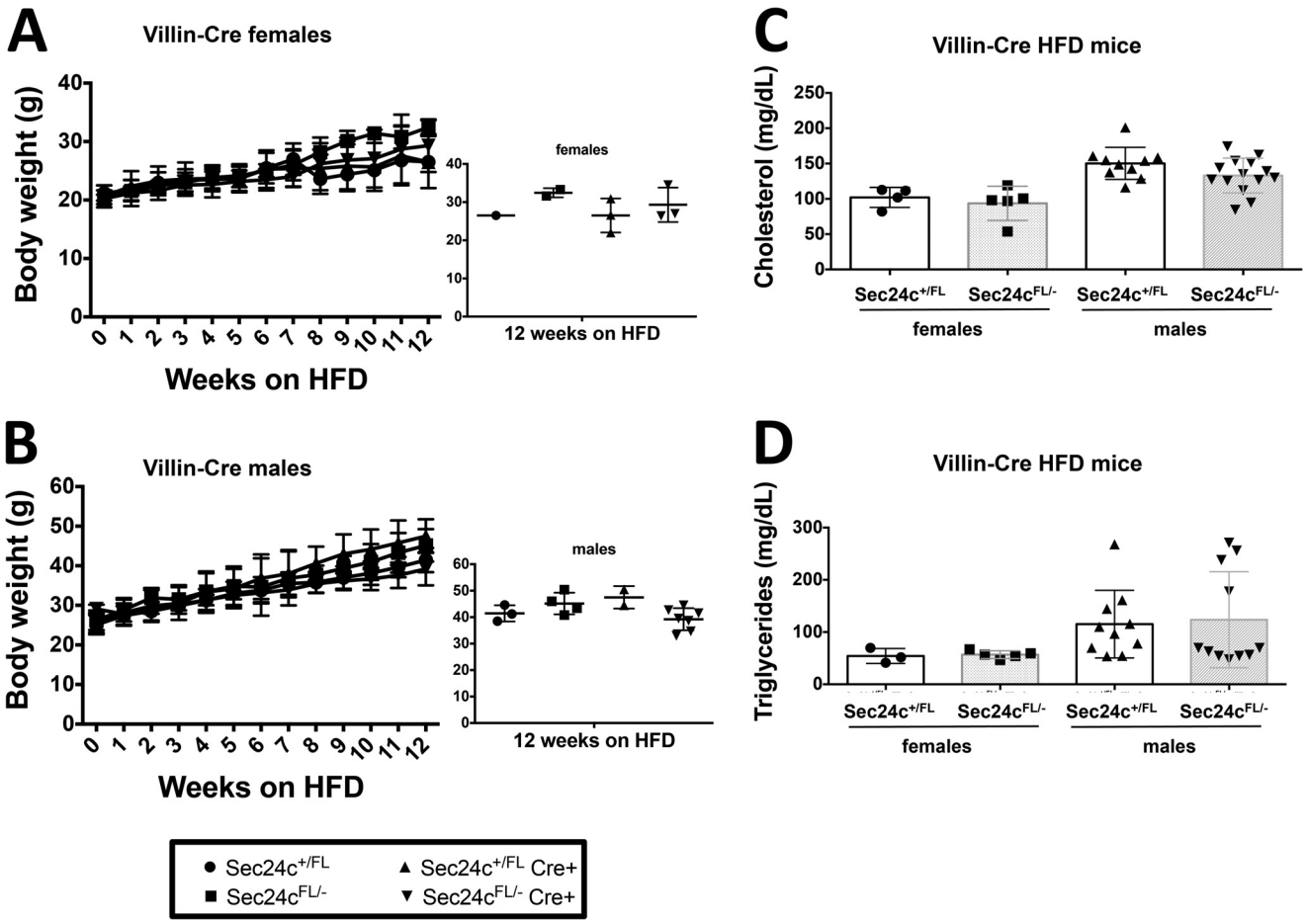

FIGURE 11. ***Sec24c$^{FL/-}$villin-Cre^{+}* mice display expected diet-induced obesity.** *Sec24c$^{FL/-}$villin-Cre^{+}* and littermate controls show no difference in weight gain over 12 weeks on HFD for females (*A*) and males (*B*), with $p > 0.05$ at all time points. Cholesterol levels (*C*) and triglyceride levels (*D*) are indistinguishable from littermate controls after 12 weeks on HFD. All *p* values >0.05 and *error bars* represent standard deviation.

NM_172596) and *Sec24c-2* (not annotated in RefSeq). The latter contains an additional in-frame exon between exons 6 and 7 encoding 23 amino acids (exon 6* in Fig. 1*A*). Although another RefSeq splice variant of *Sec24c* containing a truncated exon 4 and exon 5, as well as exon 6*, is annotated (NM_001168273.1), it was undetectable in our RT-PCR analysis.

Sec24c-2 expression is restricted to brown fat, brain, and skeletal muscle (Fig. 1, *B* and *C*) and heart, with *Sec24c-1* markedly reduced or absent in these tissues. Exon 6* and the flanking splice signals appear to be conserved in the human genome. A small number of human transcripts containing the corresponding sequence have been detected and annotated in GenBank™ (50), but it is unclear if the precise tissue-specific splice pattern is conserved. It has been reported that ~94% of human transcripts undergo alternative splicing (51). Of those transcripts, 10–30% exhibit tissue-specific alternative spicing patterns (52), with these events occurring particularly frequently in the brain, but also in skeletal muscle and the heart (53). Of note, brown fat and skeletal muscle are also thought to arise from a common progenitor (54).

The addition of in-frame exon 6* results in the insertion of 23 amino acids at the N terminus of SEC24C, just upstream of the conserved zinc finger domain. This insertion appears to be a repeat of an upstream motif, (I/L)DPD(A/S)IPSP. These residues could provide a unique binding site for a subset of cargoes expressed in these tissues. The proximity of these additional SEC24C residues to the binding site of LXM (the t-SNARE ER exit signal for syntaxin 5 and membrin) could suggest a role in regulating interactions with these or another subset of cargoes, especially given that key residues within the hypervariable region of SEC24B have been shown to compete with t-SNARE binding (18).

Our efforts to rescue the lethal *Sec24d$^{GT/GT}$* or *Sec24c$^{-/-}$* phenotype with a ubiquitous *Sec24c* or *Sec24d* transgene were unsuccessful. Although transgene mRNA expression could be detected in all or most adult tissues examined (Fig. 6*B*), the level and/or developmental timing of this expression appears to be insufficient to replace that of the endogenous *Sec24c* and *Sec24d* genes. These results are in contrast to the previously reported rescue of SEC24D-deficient mice by BAC transgenes spanning the *Sec24d* locus (20), suggesting critical regulatory element(s) present in the BAC transgenes that are absent in the chicken β-actin promoter-driven constructs. As a result, the BAC transgene likely more faithfully recapitulates the endogenous expression pattern of SEC24D (48). Despite the failure of our transgenic constructs to rescue the lethality associated with SEC24C deficiency, the health and viability of *Sec24c$^{FL/FL}$* mice (Table 2) demonstrates that the loss of *Sec24c$^{GT/GT}$* and *Sec24c$^{-/-}$* mice results from the disruption of *Sec24c* expression, either by the β-geo cassette (in *Sec24c$^{GT/GT}$* mice) or the

removal of exon 3 (in the case of the *Sec24c*$^{-/-}$ mice), rather than an effect on another locus (passenger gene) (43).

Taken together with previous reports, our data suggest a unique function for each SEC24 paralog. Although there may be overlap in cargo specificity, a subset of cargoes may require a particular mammalian SEC24 for efficient export from the ER. This specificity may be the result of intrinsic cargo selectivity among the SEC24 proteins, or alternatively, it may be a function of the particular spatio- and/or temporal expression pattern for each *Sec24* gene.

Acknowledgments—We thank Dr. Jonathan Goldberg for helpful discussions regarding the Sec24c splice forms, Marta Dzaman for help with E7.5 histology, and Anya Kiseleva and Gengeng Yu for their technical support. We acknowledge Elizabeth Hughes, Keith Childs, Galina Gavrilina, and Debora VanHeyningen for preparation of ES cell mouse chimeras from gene-trapped ES clone EPD0241-2-A11 and the Transgenic Animal Model Core of the University of Michigan's Biomedical Research Core Facilities (core support was provided by the University of Michigan Multipurpose Arthritis Center, National Institutes of Health Grant AR20557, University of Michigan Cancer Center, and National Institutes of Health Grant CA46592). All histology work was performed in the Microscopy and Image Analysis Laboratory at the University of Michigan, Biomedical Research Core Facilities, with the assistance of Judy Poore. The Microscopy and Image Analysis Laboratory is a multiuser imaging facility supported by NCI, National Institutes of Health, O'Brien Renal Center, University of Michigan Medical School, and Endowment for the Basic Sciences, Department of Cell and Developmental Biology, and the University of Michigan.

REFERENCES

1. Bonifacino, J. S., and Glick, B. S. (2004) The mechanisms of vesicle budding and fusion. *Cell* **116,** 153–166
2. Palade, G. (1975) Intracellular aspects of the process of protein synthesis. *Science* **189,** 867–867
3. Budnik, A., and Stephens, D. J. (2009) ER exit sites–localization and control of COPII vesicle formation. *FEBS Lett.* **583,** 3796–3803
4. Lee, M. C., and Miller, E. A. (2007) Molecular mechanisms of COPII vesicle formation. *Semin. Cell Dev. Biol.* **18,** 424–434
5. Zanetti, G., Pahuja, K. B., Studer, S., Shim, S., and Schekman, R. (2012) COPII and the regulation of protein sorting in mammals. *Nat. Cell Biol.* **14,** 20–28
6. Bielli, A., Haney, C. J., Gabreski, G., Watkins, S. C., Bannykh, S. I., and Aridor, M. (2005) Regulation of Sar1 NH2 terminus by GTP binding and hydrolysis promotes membrane deformation to control COPII vesicle fission. *J. Cell Biol.* **171,** 919–924
7. Lee, M. C., Orci, L., Hamamoto, S., Futai, E., Ravazzola, M., and Schekman, R. (2005) Sar1p N-terminal helix initiates membrane curvature and completes the fission of a COPII vesicle. *Cell* **122,** 605–617
8. Aridor, M., Weissman, J., Bannykh, S., Nuoffer, C., and Balch, W. E. (1998) Cargo selection by the COPII budding machinery during export from the ER. *J. Cell Biol.* **141,** 61–70
9. Kuehn, M. J., Herrmann, J. M., and Schekman, R. (1998) COPII-cargo interactions direct protein sorting into ER-derived transport vesicles. *Nature* **391,** 187–190
10. Stagg, S. M., Gürkan, C., Fowler, D. M., LaPointe, P., Foss, T. R., Potter, C. S., Carragher, B., and Balch, W. E. (2006) Structure of the Sec13/31 COPII coat cage. *Nature* **439,** 234–238
11. Miller, E., Antonny, B., Hamamoto, S., and Schekman, R. (2002) Cargo selection into COPII vesicles is driven by the Sec24p subunit. *EMBO J.* **21,** 6105–6113
12. Miller, E. A., Beilharz, T. H., Malkus, P. N., Lee, M. C., Hamamoto, S., Orci, L., and Schekman, R. (2003) Multiple cargo binding sites on the COPII subunit Sec24p ensure capture of diverse membrane proteins into transport vesicles. *Cell* **114,** 497–509
13. Nichols, W. C., Seligsohn, U., Zivelin, A., Terry, V. H., Hertel, C. E., Wheatley, M. A., Moussalli, M. J., Hauri, H. P., Ciavarella, N., Kaufman, R. J., and Ginsburg, D. (1998) Mutations in the ER-Golgi intermediate compartment protein ERGIC-53 cause combined deficiency of coagulation factors V and VIII. *Cell* **93,** 61–70
14. Zhang, B., Cunningham, M. A., Nichols, W. C., Bernat, J. A., Seligsohn, U., Pipe, S. W., McVey, J. H., Schulte-Overberg, U., de Bosch, N. B., Ruiz-Saez, A., White, G. C., Tuddenham, E. G., Kaufman, R. J., and Ginsburg, D. (2003) Bleeding due to disruption of a cargo-specific ER to Golgi transport complex. *Nat. Genet.* **34,** 220–225
15. Peng, R., De Antoni, A., and Gallwitz, D. (2000) Evidence for overlapping and distinct functions in protein transport of coat protein Sec24p family members. *J. Biol. Chem.* **275,** 11521–11528
16. Tang, B. L., Kausalya, J., Low, D. Y., Lock, M. L., and Hong, W. (1999) A family of mammalian proteins homologous to yeast Sec24p. *Biochem. Biophys. Res. Commun.* **258,** 679–684
17. Pagano, A., Letourneur, F., Garcia-Estefania, D., Carpentier, J. L., Orci, L., and Paccaud, J. P. (1999) Sec24 proteins and sorting at the endoplasmic reticulum. *J. Biol. Chem.* **274,** 7833–7840
18. Mancias, J. D., and Goldberg, J. (2008) Structural basis of cargo membrane protein discrimination by the human COPII coat machinery. *EMBO J.* **27,** 2918–2928
19. Wendeler, M. W., Paccaud, J. P., and Hauri, H. P. (2007) Role of Sec24 isoforms in selective export of membrane proteins from the endoplasmic reticulum. *EMBO Rep.* **8,** 258–264
20. Baines, A. C., Adams, E. J., Zhang, B., and Ginsburg, D. (2013) Disruption of the *Sec24d* gene results in early embryonic lethality in the mouse. *PLoS ONE* **8,** e61114
21. Richardson, L., Venkataraman, S., Stevenson, P., Yang, Y., Burton, N., Rao, J., Fisher, M., Baldock, R. A., Davidson, D. R., and Christiansen, J. H. (2010) EMAGE mouse embryo spatial gene expression database: 2010 update. *Nucleic Acids Res.* **38,** D703–D709
22. Neuhauss, S. C., Solnica-Krezel, L., Schier, A. F., Zwartkruis, F., Stemple, D. L., Malicki, J., Abdelilah, S., Stainier, D. Y., and Driever, W. (1996) Mutations affecting craniofacial development in zebrafish. *Development* **123,** 357–367
23. Driever, W., Solnica-Krezel, L., Schier, A. F., Neuhauss, S. C., Malicki, J., Stemple, D. L., Stainier, D. Y., Zwartkruis, F., Abdelilah, S., Rangini, Z., Belak, J., and Boggs, C. (1996) A genetic screen for mutations affecting embryogenesis in zebrafish. *Development* **123,** 37–46
24. Sarmah, S., Barrallo-Gimeno, A., Melville, D. B., Topczewski, J., Solnica-Krezel, L., and Knapik, E. W. (2010) Sec24D-dependent transport of extracellular matrix proteins is required for Zebrafish skeletal morphogenesis. *PLoS ONE* **5,** e10367
25. Boyadjiev, S. A., Fromme, J. C., Ben, J., Chong, S. S., Nauta, C., Hur, D. J., Zhang, G., Hamamoto, S., Schekman, R., Ravazzola, M., Orci, L., and Eyaid, W. (2006) Cranio-lenticulo-sutural dysplasia is caused by a SEC23A mutation leading to abnormal endoplasmic-reticulum-to-Golgi trafficking. *Nat. Genet.* **38,** 1192–1197
26. Schwarz, K., Iolascon, A., Verissimo, F., Trede, N. S., Horsley, W., Chen, W., Paw, B. H., Hopfner, K.-P., Holzmann, K., Russo, R., Esposito, M. R., Spano, D., De Falco, L., Heinrich, K., Joggerst, B., Rojewski, M. T., Perrotta, S., Denecke, J., Pannicke, U., Delaunay, J., Pepperkok, R., and Heimpel, H. (2009) Mutations affecting the secretory COPII coat component SEC23B cause congenital dyserythropoietic anemia type II. *Nat. Genet.* **41,** 936–940
27. Tao, J., Zhu, M., Wang, H., Afelik, S., Vasievich, M. P., Chen, X.-W., Zhu, G., Jensen, J., Ginsburg, D., and Zhang, B. (2012) SEC23B is required for the maintenance of murine professional secretory tissues. *Proc. Natl. Acad. Sci. U.S.A.* **109,** E2001–E2009
28. Chen, X.-W., Wang, H., Bajaj, K., Zhang, P., Meng, Z.-X., Ma, D., Bai, Y., Liu, H.-H., Adams, E., Baines, A., Yu, G., Sartor, M. A., Zhang, B., Yi, Z., Lin, J., Young, S. G., Schekman, R., and Ginsburg, D. (2013) SEC24A deficiency lowers plasma cholesterol through reduced PCSK9 secretion. *eLife* **2,** e00444

29. Merte, J., Jensen, D., Wright, K., Sarsfield, S., Wang, Y., Schekman, R., and Ginty, D. D. (2010) Sec24b selectively sorts Vangl2 to regulate planar cell polarity during neural tube closure. *Nat. Cell Biol.* **12,** 41–46
30. Kendall, S. K., Samuelson, L. C., Saunders, T. L., Wood, R. I., and Camper, S. A. (1995) Targeted disruption of the pituitary glycoprotein hormone α-subunit produces hypogonadal and hypothyroid mice. *Genes Dev.* **9,** 2007–2019
31. Bahou, W. F., Bowie, E. J., Fass, D. N., and Ginsburg, D. (1988) Molecular genetic analysis of porcine von Willebrand disease: tight linkage to the von Willebrand factor locus. *Blood* **72,** 308–313
32. Kawaguchi, Y., Cooper, B., Gannon, M., Ray, M., MacDonald, R. J., and Wright, C. V. (2002) The role of the transcriptional regulator Ptf1a in converting intestinal to pancreatic progenitors. *Nat. Genet.* **32,** 128–134
33. Madison, B. B., Dunbar, L., Qiao, X. T., Braunstein, K., Braunstein, E., and Gumucio, D. L. (2002) cis elements of the Villin gene control expression in restricted domains of the vertical (Crypt) and horizontal (Duodenum, Cecum) axes of the intestine. *J. Biol. Chem.* **277,** 33275–33283
34. Postic, C., Shiota, M., Niswender, K. D., Jetton, T. L., Chen, Y., Moates, J. M., Shelton, K. D., Lindner, J., Cherrington, A. D., and Magnuson, M. A. (1999) Dual roles for glucokinase in glucose homeostasis as determined by liver and pancreatic β cell-specific gene knock-outs using Cre recombinase. *J. Biol. Chem.* **274,** 305–315
35. Boucher, P., Gotthardt, M., Li, W.-P., Anderson, R. G., and Herz, J. (2003) LRP: role in vascular wall integrity and protection from atherosclerosis. *Science* **300,** 329–332
36. Tallquist, M. D., and Soriano, P. (2000) Epiblast-restricted Cre expression in MORE mice: a tool to distinguish embryonic *vs.* extra-embryonic gene function. *Genesis* **26,** 113–115
37. Van Keuren, M. L., Gavrilina, G. B., Filipiak, W. E., Zeidler, M. G., and Saunders, T. L. (2009) Generating transgenic mice from bacterial artificial chromosomes: transgenesis efficiency, integration and expression outcomes. *Transgenic Res.* **18,** 769–785
38. Fahim, A. T., Wang, H., Feng, J., and Ginsburg, D. (2009) Transgenic overexpression of a stable plasminogen activator inhibitor-1 variant. *Thromb. Res.* **123,** 785–792
39. Alexopoulou, A. N. (2008) The CMV early enhancer/chicken β actin (CAG) promoter can be used to drive transgene expression during the differentiation of murine embryonic stem cells into vascular progenitors. *BMC Cell Biol.* **9,** 2
40. Hitoshi, N., Kenichi, Y., and Junichi, M. (1991) Efficient selection for high-expression transfectants with a novel eukaryotic vector. *Gene* **108,** 193–199
41. Nagy, A., Gertsenstein, M., Vintersten, K., and Behringer, R. (2003) *Manipulating the Mouse Embyro: A Laboratory Manual*, pp. 237–319, Cold Spring Harbor Laboratory Press, Cold Spring Harbor, NY
42. Krupp, M., Marquardt, J. U., Sahin, U., Galle, P. R., Castle, J., and Teufel, A. (2012) RNA-Seq Atlas, a reference database for gene expression profiling in normal tissue by next-generation sequencing. *Bioinformatics* **28,** 1184–1185
43. Westrick, R. J., Mohlke, K. L., Korepta, L. M., Yang, A. Y., Zhu, G., Manning, S. L., Winn, M. E., Dougherty, K. M., and Ginsburg, D. (2010) A spontaneous Irs1 passenger mutation linked to a gene targeted SerpinB2 allele. *Proc. Natl. Acad. Sci. U.S.A.* **107,** 16904–16909
44. Frutkin, A. D., Shi, H., Otsuka, G., Levéen, P., Karlsson, S., and Dichek, D. A. (2006) A critical developmental role for tgfbr2 in myogenic cell lineages is revealed in mice expressing SM22-Cre, not SMMHC-Cre. *J. Mol. Cell. Cardiol.* **41,** 724–731
45. Jones, B., Jones, E. L., Bonney, S. A., Patel, H. N., Mensenkamp, A. R., Eichenbaum-Voline, S., Rudling, M., Myrdal, U., Annesi, G., Naik, S., Meadows, N., Quattrone, A., Islam, S. A., Naoumova, R. P., Angelin, B., Infante, R., Levy, E., Roy, C. C., Freemont, P. S., Scott, J., and Shoulders, C. C. (2003) Mutations in a Sar1 GTPase of COPII vesicles are associated with lipid absorption disorders. *Nat. Genet.* **34,** 29–31
46. Sucic, S., El-Kasaby, A., Kudlacek, O., Sarker, S., Sitte, H. H., Marin, P., and Freissmuth, M. (2011) The serotonin transporter is an exclusive client of the coat protein complex II (COPII) component SEC24C. *J. Biol. Chem.* **286,** 16482–16490
47. Bengel, D., Murphy, D. L., Andrews, A. M., Wichems, C. H., Feltner, D., Heils, A., Mössner, R., Westphal, H., and Lesch, K.-P. (1998) Altered brain serotonin homeostasis and locomotor insensitivity to 3,4-methylenedioxymethamphetamine ("Ecstasy") in serotonin transporter-deficient mice. *Mol. Pharmacol.* **53,** 649–655
48. Yang, X. W., and Gong, S. (2005) An overview on the generation of BAC transgenic mice for neuroscience research. *Curr. Protoc. Neurosci.* **31,** 5.20.1–5.20/11
49. Pruitt, K. D., Tatusova, T., and Maglott, D. R. (2005) NCBI Reference Sequence (RefSeq): a curated non-redundant sequence database of genomes, transcripts and proteins. *Nucleic Acids Res.* **33,** D501–D504
50. Benson, D. A., Cavanaugh, M., Clark, K., Karsch-Mizrachi, I., Lipman, D. J., Ostell, J., and Sayers, E. W. (2013) GenBank. *Nucleic Acids Res.* **41,** D36–D42
51. Wang, E. T., Sandberg, R., Luo, S., Khrebtukova, I., Zhang, L., Mayr, C., Kingsmore, S. F., Schroth, G. P., and Burge, C. B. (2008) Alternative isoform regulation in human tissue transcriptomes. *Nature* **456,** 470–476
52. Xu, Q., Modrek, B., and Lee, C. (2002) Genome-wide detection of tissue-specific alternative splicing in the human transcriptome. *Nucleic Acids Res.* **30,** 3754–3766
53. Chen, M., and Manley, J. L. (2009) Mechanisms of alternative splicing regulation: insights from molecular and genomics approaches. *Nat. Rev. Mol. Cell Biol.* **10,** 741–754
54. Seale, P., Bjork, B., Yang, W., Kajimura, S., Chin, S., Kuang, S., Scimè, A., Devarakonda, S., Conroe, H. M., Erdjument-Bromage, H., Tempst, P., Rudnicki, M. A., Beier, D. R., and Spiegelman, B. M. (2008) PRDM16 controls brown fat/skeletal muscle switch. *Nature* **454,** 961–967